Fabric defect detection by Fourier analysis

Chi-ho Chan and Grantham Pang
Dept. of Electrical and Electronic Engineering
The University of Hong Kong
Pokfulam Road
Hong Kong
Fax: (852)-2559-8738
Phone: (852)-2859-2689
Email: ***chichan@eee.hku.hk***

Abstract - **Many fabric defects are very small and undistinguishable, which are very difficult to detect by only monitoring the intensity change. Faultless fabric is a repetitive and regular global texture and Fourier transform can be applied to monitor the spatial frequency spectrum of a fabric. When a defect occurs in fabric, its regular structure is changed so that the corresponding intensity at some specific positions of the frequency spectrum would change. However, the three-dimensional frequency spectrum is very difficult to analyze. In this paper, a simulated fabric model is used to understand the relationship between the fabric structure in the image space and in the frequency space. Based on the three-dimensional frequency spectrum, two significant spectrum diagrams are defined and used for analyzing the fabric defect. These two diagrams are called the central spatial frequency spectrums. The defects are broadly classified into four classes: (1) double yarn; (2) missing yarn; (3) webs or broken fabric; and (4) yarn densities variation. After evaluating these four classes of defects using some simulated models and real samples, seven characteristic parameters for central spatial frequency spectrum are extracted for defect classification.**

I. INTRODUCTION

In the textile industry, before any shipment to customers, inspection is needed for maintaining the fabric quality. Srinivasan et. al.[1] have stated that the price of second-quality fabric is only 45 to 65% of that of first-quality fabric. However, the current inspection process still depends mainly on human sight. This nature of work is very dull and repetitive. Moreover, there could be many human errors in this process. According to some studies, human visual inspection can only catch around 60% to 75% of the significant defects [2]. Therefore, in order to lower the cost of the inspection process and to increase the competitive advantage of the products, it is necessary to automate the inspection process.

In this study, the central spatial frequency spectrum approach is introduced and examined. This method would reduce the computational time for defect detection and provide more parameters for defect classification. Before introducing this method, the characteristics of fabric structure in frequency spectrum will be examined and some defect examples will be described. After that, the procedures of the method and experimental results will be discussed.

Zhang et. al. [3] have introduced two approaches to detect defects: gray level statistical and morphological methods. Lanes [4] has defined a number of convolution masks to detect the defect. These methods, which depend on intensity change on the fabric image, can only capture the significant defects such as knot, web and slub. However, faultless fabric has a periodic regular global structure. The occurrence of a defect in the fabric means that the regular structure has been destroyed. Therefore, the fabric defect can be detected by monitoring fabric structure. C.Ciamberllini and his colleagues have used the optical Fourier transform to monitor the fabric structure. Their methods can be classified as follows: fixed masks or structured detectors, adaptable filters [5], electronic elaboration of the image [6], and binary histogram [7]. Fixed masks, structured detectors and adaptive filters are the fixed optical filters placed over the photodetector active area. They are composed of periodic array transparent and opaque zones, and their locations depend on the peak of the fabric diffraction image. When a defect occurs, some localized peaks in the diffraction image will be passed to the sensor. However, this type of operation requires a careful alignment and different fabric type requires different filter. The method of electronic elaboration is based on the subtraction of the reference image of faultless fabric from that of the fabric under inspection. The binary histogram method is based on a summation of the gray level pixels, which have gray level greater than a threshold. The threshold is defined according to the fabric type and system sensitivity. Anyhow, optical processing is very expensive and requires careful calibration. Also, this method could not recognize fabric with higher fabric density.

Another class of method is dependent on digital image processing. Wood [8] has used Fourier and associate transform to characterize carpet patterns. Ravandi and Toriumi [9] have used Fourier transform analysis to measure fabric appearance. Fabric surface characteristics, fill and warp yarns for plain-weave cotton fabric were also discussed. Escofet et. al. [10] have used the angular correlation of the Fourier spectra to evaluate fabric web resistance to abrasion. Sari-Saraf and his colleagues [11] have used Fourier transform to detect fabric defects. Their approach examines and performs a one-dimensional signature in the two-dimensional spectrum. The signature is obtained by integrating the points within each ring in the two-dimensional spectrum. The rings are concentric with different radii, and they are used to monitor the fill and wrap densities. The idea

0-7803-5589-X/99/$10.00 © 1999 IEEE

of this approach is similar to the concentric ring filter in optical processing [5]. The main advantage of this approach is that it is less sensitive to the background noise (intensity source variation). Also, it is more effective for revealing a defect due to dimensional changes in the structure of the fabric. This method can recognize the high fabric densities by using the zoomed camera, but long computational time is expected.

II. Background Knowledge

A. Fourier Transform

Fourier theorem states that any signal can be represented by the sum of the sine and cosine wave with various amplitudes and frequencies. That is, the relationship between a repetitive, regular and uniform fabric pattern in the image space and its spectrum in the spatial frequency can be linked by operating two-dimensional Fourier transform. Let a two-dimensional image be $f(x,y)$, which is a real function representing the gray level in x, y spatial coordinates, and let the image width and image length be N. Then $F(n,m)$ denotes the Fourier transform of $f(x,y)$ with n and m spatial frequencies. The general equation of two-dimensional discrete Fourier transform is shown below.

$$F(n,m)=\frac{1}{N^2}\sum_{y=0}^{N-1}\sum_{x=0}^{N-1} f(x,y)*e^{-j2\pi(xn+ym)/N} \qquad (1)$$

The computational time for Fourier transform is generally long. For two-dimensional discrete Fourier transform, it is proportional to the second order of the image size. In order to reduce the computation time, Fast Fourier transform (FFT) is used. Fast Fourier transform is a discrete Fourier transform with some reorganization that can save enormous amount of time. For one-dimensional FFT, the computation time is $N\log_2 N$. Because of the separable transform [12] being used to perform the two-dimensional transform, the computation time is proportional to $2N^2\log_2 N$. One of the advantages for the spatial frequency spectrum approach is the translation property of Fourier transform [12] that is shown in (2), which means that the magnitude of frequency spectrum does not change when the fabric is moved up. The spectrum is only varied by the change of fabric structure.

$$f(x-a,y-b)\Leftrightarrow F(f_x,f_y)*e^{-j2\pi(Mf_x a+Nf_y b)/MN} \qquad (2)$$

B. Characteristics of Fabric Structure in the Magnitude of Frequency Spectrum

A simulated frequency spectrum should be examined for understanding the characteristics of fabric structure in the magnitude of frequency spectrum. Two-dimensional discrete convolution theorem is involved for constructing a simulated fabric. Let h and g be the input and output image respectively, and t is a convolution mask. Therefore, the convolution denoted by $\otimes$ is the computation of weighted sums of the image pixels with the convolution mask, which is shown in (3).

$$g(x,y)=t(x,y)\otimes h(x,y)$$
$$=\sum_{\tau_1=0}^{x}\sum_{\tau_2=0}^{y} t(\tau_1,\tau_2)h(x-\tau_1,y-\tau_2) \qquad (3)$$

The simulated pattern of a faultless fabric is shown in Figure 1(c). The faultless fabric image pattern, $f(x,y)$, is modeled as shown in (4) below.

$$f(x,y)=rect(x/s_x,y/s_y)\otimes\sum_{n_1=-\infty}^{\infty}\sum_{n_2=-\infty}^{\infty}\delta(x-n_1w_x,y-n_2w_y) \qquad (4)$$

where

$$rect(u,v)=\begin{cases}1 & |u|\le 0.5 \text{ and } |v|\le 0.5\\ 0 & \text{otherwise}\end{cases}$$

where $\delta(u,v)=\delta(u)\delta(v)$, which is the two-dimensional Dirac δ function.

The first part is a function that describes the fabric structure gap (Figure 1(a)), where s_x is the width of the gap and s_y is the height of the gap. Let w_x be the wrap period and w_y be the fill period. The second part is the impulse function that models the location of the gap in the fabric (Figure 1(b)).

The Fourier transform of the convolution of two functions in an image space is equal to the product of their respective Fourier transforms as shown in (5) below.

$$|F(f_x,f_y)|=\left|s_x\cdot s_y\cdot sinc(2\pi f_x\cdot s_x)\cdot sinc(2\pi f_y\cdot s_y)\cdot\left[\frac{4\pi^2}{w_x\cdot w_y}\sum_{n_1=-\infty}^{\infty}\sum_{n_2=-\infty}^{\infty}\delta\left(2\pi f_x-\frac{2\pi n_1}{w_x},2\pi f_y-\frac{2\pi n_2}{w_y}\right)\right]\right| \qquad (5)$$

The frequency spectrums of the corresponding figures of Figure 1 are shown in Figure 2. The envelope of the faultless fabric in frequency space shown in Figure 2(c) is proportional to the envelope of the Fourier transform of the fabric structure gap as shown in Figure 2(a). In fact, the shape of the envelope of Figure 2(a) is affected by two parameters: s_x and s_y. For example, if the structure gap s_x and s_y are increased, the envelope shape of Figure 2(a) will be narrower. Referring to Figure 1(b), the location of the impulse in the image space is inversely proportional to the impulse location in frequency space in Figure 2(b). The distance between two impulses in Figure 2(b) should be $1/w_x$ in the horizontal axis and $1/w_y$ in the vertical axis. These properties can aid to monitor the yarn densities in the two directions. For example, the density in the horizontal direction is equal to the distance between two impulses in the horizontal axis (i.e. $1/w_x$) multiplies with the image width.

C. Simulation of Fabric Defect

In this paper, the defects are broadly classified into four classes: (1) double yarn; (2) missing yarn; (3) webs or broken fabric; and (4) yarn densities variation. Examples are shown in Figure 3. The double yarn (fill) is a change of spatial periodicity on the vertical axis. The spectrum on the f_x-axis (fill direction) denotes the corresponding change of spatial

frequency. In a simulated model of the double yarn, $D(x,y)$, shown in Figure 4(c), the defect can be regarded as a subtraction from a faultless fabric (Figure 4(a)) to a series of rectangle function, $d(x,y)$ (Figure 4(b)). Because of the distributivity property of the Fourier transform,

$$F\{D(x,y)\} = F\{f(x,y) - d(x,y)\} = F\{f(x,y)\} - F\{d(x,y)\} \quad (6)$$

which means that the defect in the frequency space can be formed by subtracting the faultless fabric frequency spectrum to the Fourier transform of an irregular structure function $d(x,y)$.

D. Central Spatial Frequency Spectrum

Due to the nature of the fabric structure, many defects would occur along the x and y-axes, which means that those characteristics would appear on the wrap (f_y) and fill (f_x) direction in the frequency spectrum. In addition, a three-dimensional graph of the frequency spectrum is very difficult to analyze. The method of central spatial frequency spectrum is therefore proposed in this paper. This method extracts two diagrams along the f_x and f_y direction ($|F(f_x,0)|$ and $|F(0,f_y)|$) from the three-dimensional graph, which are shown in Figure 5.

Seven significant features can be extracted in these two diagrams for describing defect characteristics. The equations of these parameters are shown below.

$$P1 = F(0,0) \qquad P2 = 100 \times F(f_{x1},0)/F(0,0)$$

$$P3 = f_{x1} \qquad P4 = 100 \times \left(\sum_{f_{xi}=0}^{f_{x1}} F(f_{xi},0) \Big/ F(0,0) \right)$$

$$P5 = 100 \times F(0,f_{y1})/F(0,0) \qquad P6 = f_{y1}$$

$$P7 = 100 \times \left(\sum_{f_{yi}=0}^{f_{y1}} F(0,f_{yi}) \Big/ F(0,0) \right)$$

where f_{x1} and f_{y1} correspond to the first harmonic frequency in their respective diagrams that are also shown in Figure 5. The first feature **P1** is the average light intensity of the image, which is used to characterize the yarn density. Higher yarn density decreases the light intensity and **P1** is decreased, and vise versa. **P5**, **P6**, **P7** are used to monitor the wrap (vertical) threads structure whereas **P2**, **P3** and **P4** are for detecting the fill (horizontal) threads structure. When defects occur, the amplitude of harmonic frequencies plus other changes would appear in the central spatial frequency spectrum. Features **P2, P4, P5** and **P7** are used to describe and detect these characteristics. Feature **P3** and **P6** are used to monitor the wrap and fill threads density in the image. Those features are more concentrated on analyzing the region between the central peak and first peak (first harmonic frequency) because higher harmonic frequency components are significantly distorted in real environment.

A defect such as double wrap is shown in Figure 6(a). A comparison of the defect spectrum and faultless fabric spectrum are shown in Figure 6(b and c), where the defect is denoted by the solid line and the faultless fabric is denoted by the crosses. Both Figure 6(b and c) show that the central peak value (**P1**) of the defect fabric is lower than that of the faultless fabric. This is because one or more vertical (Wrap) threads are added in the faultless fabric, which leads to be lower light intensity in the defect image. The double wrap defect is a change of spatial periodicity in the horizontal axis, and therefore the $|F(0,f_y)|$ diagram is changed mostly. In this diagram (Figure 6 (c)), the first peak value of the defect at f_{y1} $=35$ are lower than the faultless fabric first peak values and ripples occur. So **P5** should be lower and **P7** should be higher. The first peak location (**P6**= f_{y1} $=35$) is a fundamental yarn frequency, which means that the peak location is proportional to the yarn density. In this example, **P6** is almost unchanged. A summary is shown in the second row of table 1. With a similar interpretation, the double fill defect is a change of spatial periodicity in the vertical axis. Hence, the parameters **P2** and **P4** are changed because the defect only affects the $|F(f_x,0)|$ diagram.

The difference between missing yarn and double yarn is their fabric threads count. Average light intensity **P1** can show this characteristic. For missing yarn, higher **P1** is expected because there is less thread in this defect. Broken fabric and yarn densities variation are a change of periodicity in both x and y axis, and both $|F(f_x,0)|$ and $|F(0,f_y)|$ diagrams are mostly changed. **P3** and **P6** values are not changed in the broken fabric. This is because this defect is a instant change of the fabric density, and it only affects **P1, P2, P4, P5** and **P7** values. The **P1** is high because the fabric is broken, and leads to increase of light intensity. Details of the expected results are summarized below.

TABLE 1
DIFFERENCE IN PARAMETERS PREDATED BETWEEN THE FABRIC AND ITS DEFECT

	P1	P2	P3	P4	P5	P6	P7
Double (Fill) yarn	L	L	NC	H	NC	NC	NC
Double (Wrap) yarn	L	NC	NC	NC	L	NC	H
Missing (Fill) yarn	H	L	NC	H	NC	NC	NC
Missing (Wrap) yarn	H	NC	NC	NC	L	NC	H
Broken Fabric	H	L	NC	H	L	NC	H
Low fabric density	H	L	L	L	L	L	H
High fabric density	L	L	H	L	L	H	L

H: Higher, L: Lower, NC: no change.

III. EXPERIMENTAL SETUP

A. Image Acquisition

In this study, plain white fabrics are used. Defects with double yarn, missing yarn, web and fabric density variation were inspected and compared with the faultless fabric. The image acquisition system includes a personal computer (Pentium-200MMX), frame grabber, cmos-imager and a system monitor. The fabric image is captured by a cmos-imager, and a frame grabber digitizes the video signal into a 768*576 pixel with eight-bit gray level resolutions image and

stores it into computer memory. This image data is then processed by the defect detection procedures as shown in Figure 7. Backlighting illumination is used to achieve the high contrast fabric images.

B. Histogram Equalization

Histogram equalization is performed to obtain a uniform density image histogram [12]. This process extends the dynamic range of gray levels and increases the image contrast. The aim is to standardize the brightness and contrast of the images. Figure 8 gives an example of using equalization to improve the overall brightness and contrast of an image.

C. Fast Fourier Transform

A Fast Fourier Transform (two-point) transform is used [12] for fast computation, which means that the image size is cut to 512X512 pixels in our experiment. This is because the image length and width should be a power of two. A software package, Matlab, is used for this experiment. After the Fourier transform, the central spatial frequency spectrum diagram is extracted from the three-dimensional diagram. A real sample of double fill and its central spatial frequency spectrum diagrams are shown in Figure 9(b, c and d).

By observing these two diagrams (Figure 9(c and d)) and comparing them with the simulated diagrams of double wrap in Figure 6(b and c), the orientation of the defect mainly affects the particular diagram. For example, double wrap affects the parameters in $|F(0,f_y)|$ diagram, and double fill only affects the parameters in $|F(f_x,0)|$ diagram. However, the high spatial frequency peaks in Figure 9(b and c) are loosely localized and embedded with some noise. A number of reasons can explain this result. For example, the surface tufts give a random textured component in the fabric images that distort the periodic structure. In addition, the illumination fluctuation gives high frequencies noise background. Because of these effects, only parameters around the central peaks and the first peaks can be extracted for defect characteristics.

IV. RESULTS

The negative parameter in the table means that the particular characteristic of the defect spectrum pattern is lower than that of the faultless fabric. In this experiment, four defect models and the four corresponding real samples are used to examine this approach. Table 2 gives the difference in parameters obtained between simulated fabric and its defect. The results in table 2 follows our expectation summarized earlier in table1.

TABLE 2
DIFFERENCE IN PARAMETERS OBTAINED BETWEEN A SIMULATED FABRIC MODEL AND ITS DEFECT.

	P1	P2	P3	P4	P5	P6	P7
Double (Wrap) yarn	**-2.1** (L)	0 (NC)	0 (NC)	0 (NC)	**-14.4** (L)	**0** (NC)	**66.7** (H)
Missing (Wrap) yarn	**2.9** (H)	0 (NC)	0 (NC)	0 (NC)	**-5.3** (L)	**0** (NC)	**71.8** (H)
Broken Fabric (Web)	**33.4** (H)	**-14.9** (L)	**0** (NC)	**32.95** (H)	**-24.2** (L)	**0** (NC)	**25.5** (H)
Low fabric density	**32.2** (H)	**-17** (L)	**-8** (L)	**-0.8** (L)	**-25.3** (L)	**-6** (L)	**19.9** (H)

TABLE 3
DIFFERENCE IN PARAMETERS OBTAINED BETWEEN A REAL FABRIC AND ITS DEFECT.

	P1	P2	P3	P4	P5	P6	P7
Double (fill) yarn	**-0.1** (L)	**-4.5** (L)	**0** (NC)	**19** (H)	-0.3 (NC)	0 (NC)	2 (NC)
Missing (Wrap) yarn	**5.1** (H)	0.6 (NC)	0 (NC)	-7.8 (NC)	**-3.1** (L)	**0** (NC)	**14.9** (H)
Broken Fabric (Web)	**6.5** (H)	**-11.2** (L)	**-1** (NC)	**-0.9** (H)	**-4.3** (L)	**-6** (NC)	**2.9** (H)
High fabric density	**-4.6** (L)	**-10.3** (L)	**18** (H)	**-12.4** (L)	**-1.6** (L)	**15** (H)	**18.8** (L)

Missing Wrap is an example for describing these parameters. Since this defect is missing one or more vertical threads, it only occurs in $|F(0,f_y)|$ diagram. Therefore, the significant parameters should be **P1**, **P5**, **P6** and **P7**. Since the fabric thread count is lower than the faultless fabric, the average light intensity of defect is higher. Due to this reason, **P1** should therefore be higher. In addition, due to the irregular texture in the wrap direction, the first peak value is decreased and ripple occurs, which would cause **P5** lower and **P7** higher. However, because of the noise effects on the real samples that are mentioned in the previous section, the parameters in table 3 are distorted. Anyway, those changed parameters from the real samples are quite similar to the simulated parameters. Moreover, the bolded parameters in table 2 and table 3 show that different classes of defects have their own changed parameters, which means that these seven parameters can be used to classify the fabric defect type.

V. CONCLUSIONS

The Fourier transform approach is described to detect the structural defect. The simulated models are used to understand the behavior of frequency spectrum. Since the three-dimensional frequency spectrum is very difficult to analyze and many defects occur along the horizontal and vertical axes, the central spatial frequency spectrum approach has been proposed to increase the efficiency of the analysis process. Seven significant characteristic parameters can be extracted from the central spatial frequency spectrums for describing the defect type. Experiments have shown that the extracted parameters can be used to classify fabric defects.

REFERENCES

[1] K.Srinivasan, P.H. Dastoor, P.Radhakrishnaiah and S. Jayaraman, "FDAS: A Knowledge-based Framework for Analysis of Defects in Woven Textile Structures", *J. Text. Inst.*, vol. 83, Part 1, no. 3, pp.431-1448 (1992).

[2] K. Schicktanz, "Automatic fault detection possibilities on nonwoven fabrics," *Melliand Textilberichte*, pp. 294-295, (1993).

[3] X. F. Zhang and R. R. Bresee, "Fabric Defect Detection and classifiction using Image Analysis," *Textile Research Journal,* vol. 65(1), pp.1-9, (1995).
[4] J. S. Lane, S.C. Moure, "Textile fabric Inspection System," *US Patent No. 5,774,177* (1998).
[5] C. Ciamberlini, F. Francini, P. Sansoni and B. Tiribilli, "Defect detection in textured materials by optical filtering with structured detectors and self-adaptable masks", *Opt. Eng.*, vol. 35(3), pp. 838-844, (1996).
[6] C. Castellini, F. Francini, G. Longobardi and B. Tiribilli, "On-line Textile Quality Control using Optical Fourier Transforms," *Optics and Lasers in Engineering*, vol. 24, pp. 19-32 (1996).
[7] C. Ciamberlini, F. Francini, G. Longobardi, P. Poggi, P. Sansoni and B. Tiribilli, "Weaving defect detection by Fourier Imaging," *Vision systems in applications SPIE*, vol. 2786, pp. 9-18 (1996).
[8] E. J. Wood, "Applying Fourier and associated transforms to Pattern Characterization in Textiles," *Textile Research Journal,* pp.212-220, (1990).
[9] S.A.H. Ravandi and K. Toriumi, "Fourier Transform Analysis of plain Weave Fabric Appearance," *Textile Research Journal*, vol. 65(11), pp. 676-683 (1995).
[10] J. Escofet, M.S. Millan, H. Abril and E. Torrecilla, "Inspection of fabric resistance to abrasion by fouries analysis," *Proc. SPIE* , vol. 3490, pp. 207-210 (1998).
[11] H. Sari-Saraf and J. S. Goddard, "On-line optical measurement and monitoring of yarn density in woven fabrics," *Automated Optical Inspection for Industry, SPIE*, vol. 2899, pp. 444-452 (1996).
[12] R. C. Gonzalez and R.E. Woods, "Image transforms", Chap.3 and "Image enchancement", Chap.4 in *Digital Image Processing,* Addison-Wesley, pp.81-128, 166-189 (1993).

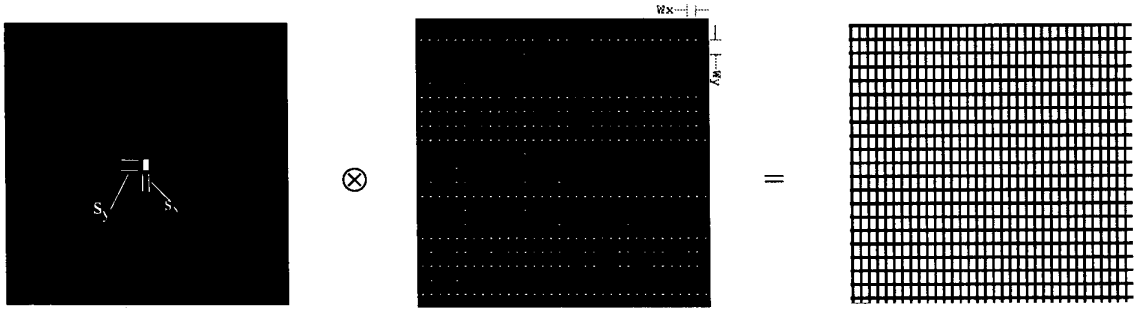

(a) (b) (c)

Figure 1(a) Fabric structure gap. (b) Fabric gap location. (c) Simulated faultless fabric

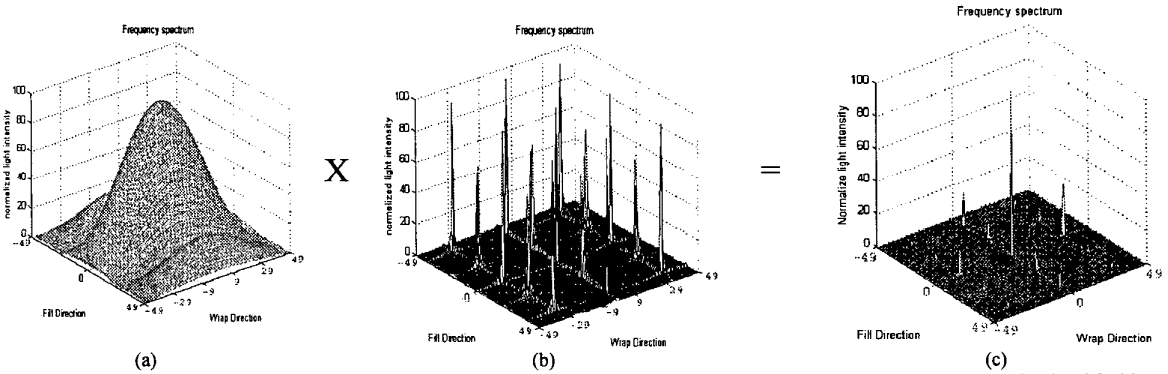

(a) (b) (c)

Figure 2. Magnitude of frequency spectrum (Central portion): (a) Fabric structure gap, (b) fabric gap location, (c) simulated faultless fabric.

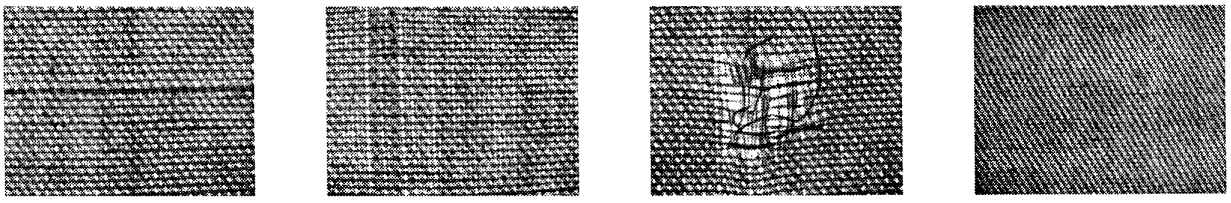

(a) (b) (c) (d)

Figure 3 Fabric defect samples: (a) Double yarn; (b) Missing yarn; (c) Broken fabric; (d) Variation of yarn.

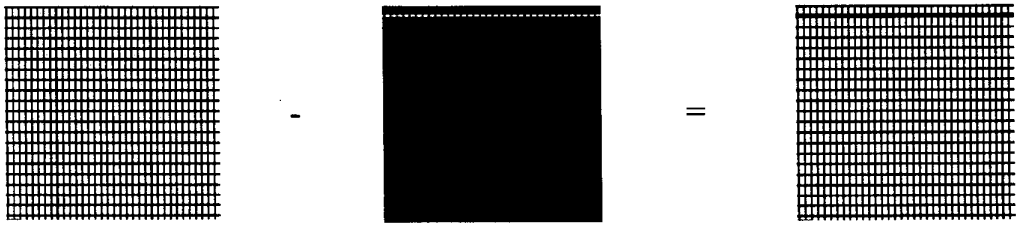

(a) (b) (c)

Figure 4 (a) Faultless fabric $f(x,y)$, (b) Rectangle series function $d(x,y)$, (c) Double fill defect

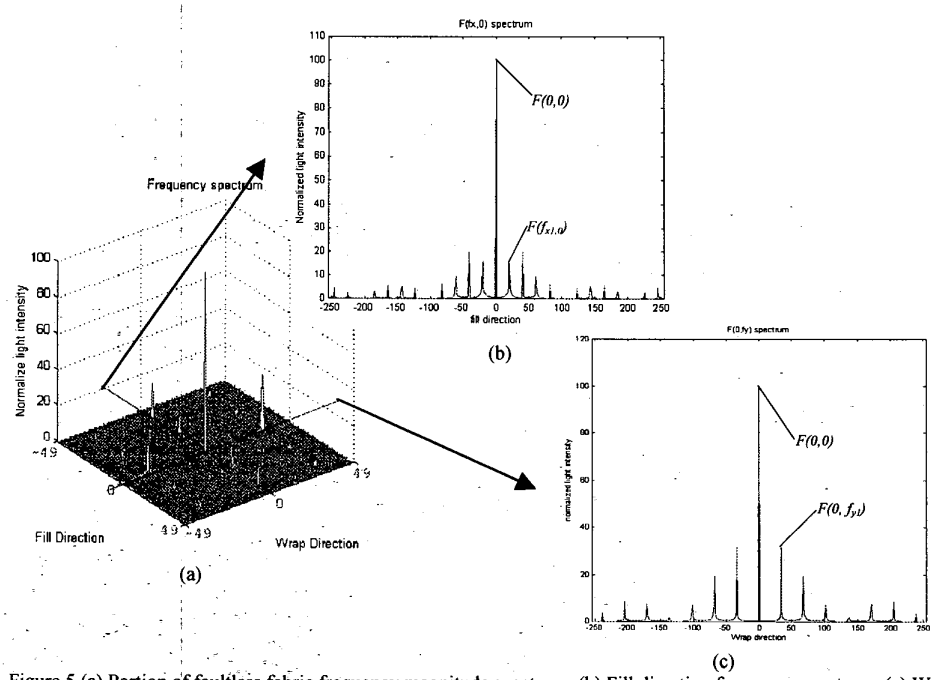

Figure 5 (a) Portion of faultless fabric frequency magnitude spectrum. (b) Fill direction frequency spectrum, (c) Wrap direction frequency spectrum

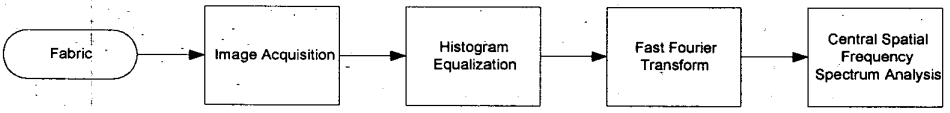

Figure 7 System flow of Fabric defect detection

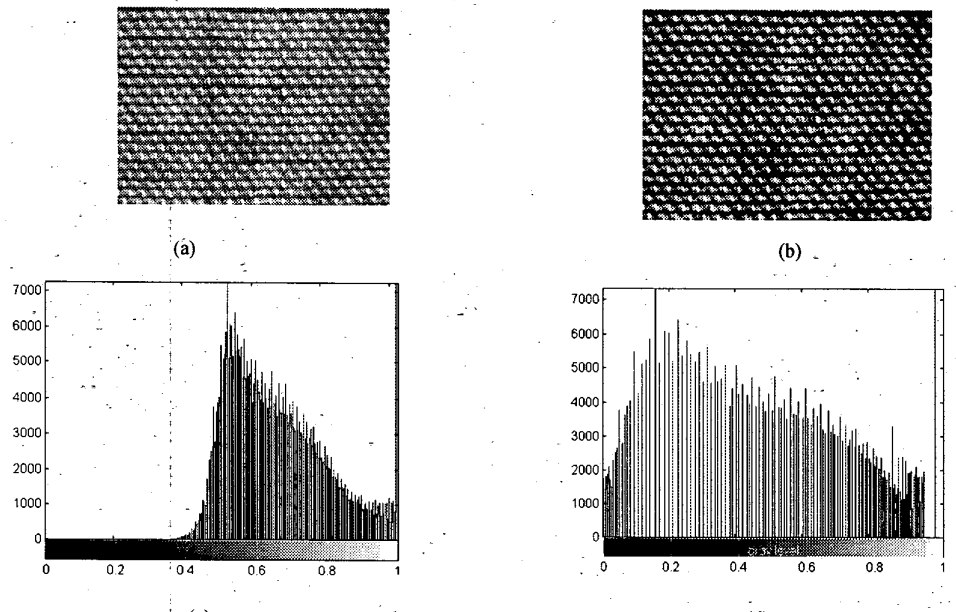

Figure 8 Example of an image with gray level histogram:
(a) original image and (b) gray level histogram (c) image after equalization and (d) gray level histogram after equalization.

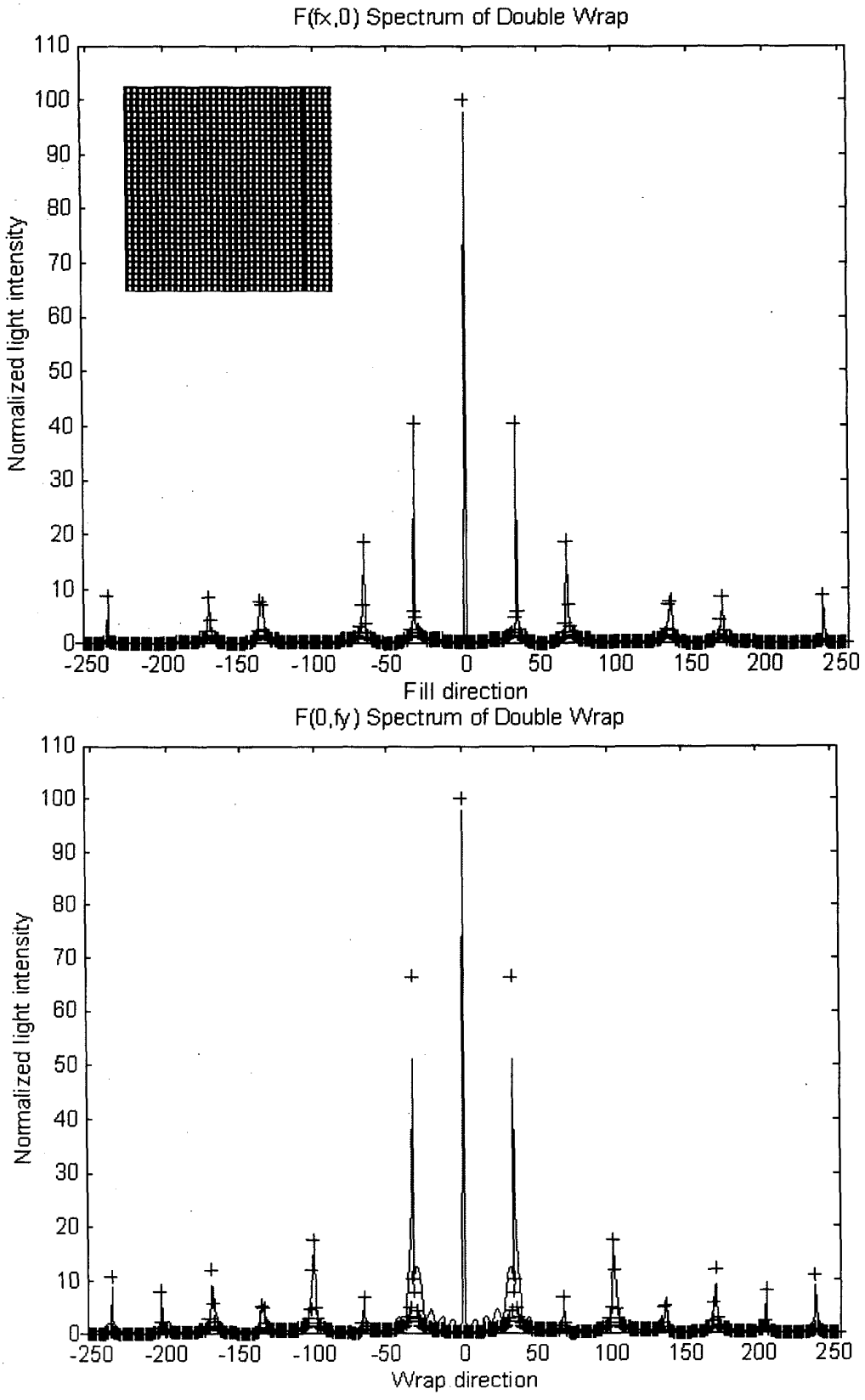

Figure 6 (a) Double yarn, (b) its fill direction spectrum, (c) its wrap direction spectrum.

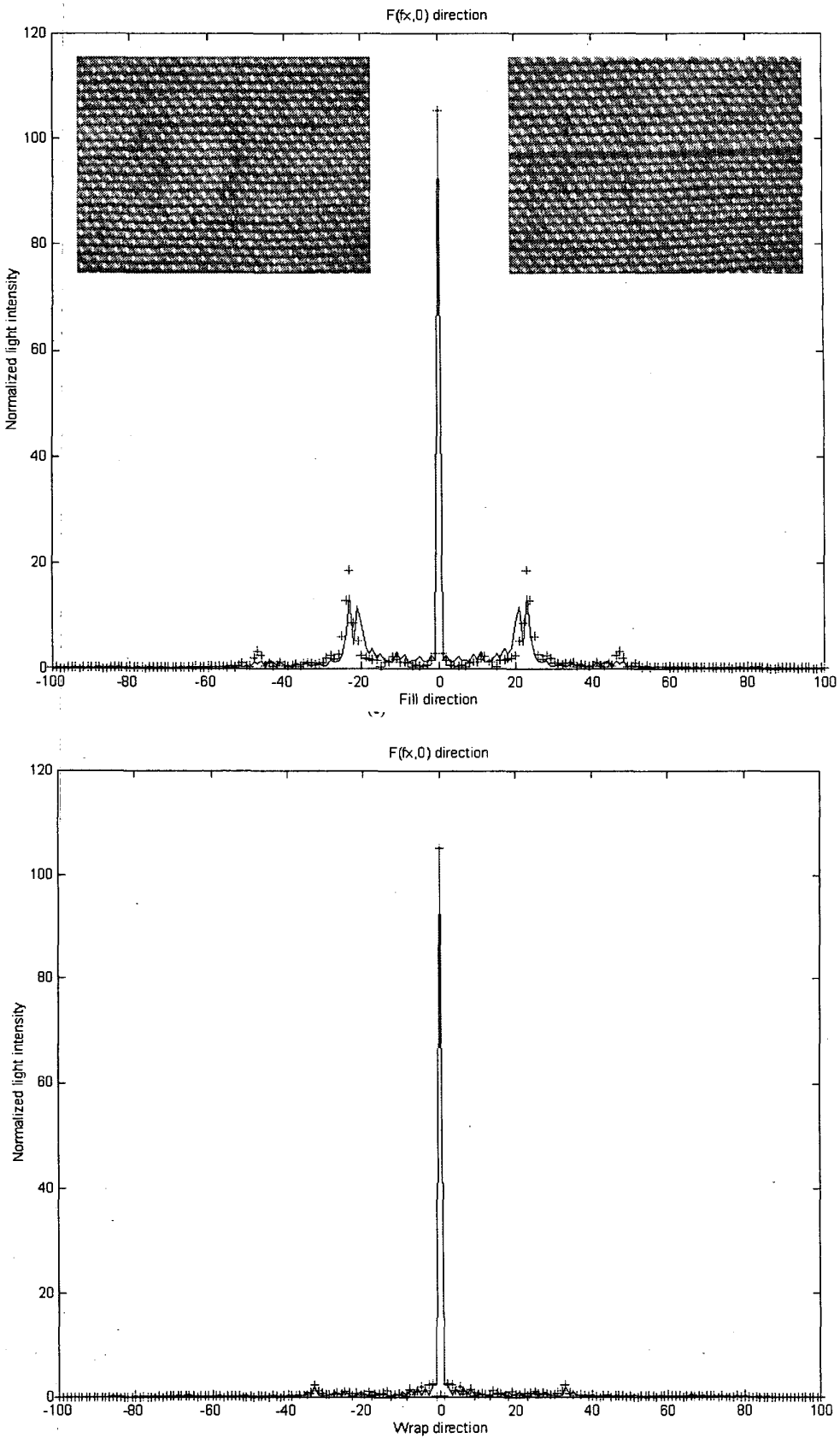

Figure 9 (a) faultless fabric, (b) double fill, (c) their fill direction spectrum, (d) their wrap direction spectrum.